

Extended megadroughts in the southwestern United States during Pleistocene interglacials

Peter J. Fawcett¹, Josef P. Werne^{2,4,5}, R. Scott Anderson^{6,7}, Jeffrey M. Heikoop⁸, Erik T. Brown³, Melissa A. Berke³, Susan J. Smith⁷, Fraser Goff¹, Linda Donohoo-Hurley¹, Luz M. Cisneros-Dozal⁸, Stefan Schouten⁹, Jaap S. Sinninghe Damsté⁹, Yongsong Huang¹⁰, Jaime Toney⁸, Julianna Fessenden⁶, Giday WoldeGabriel⁶, Viorel Atudorei¹, John W. Geissman¹ & Craig D. Allen¹¹

The potential for increased drought frequency and severity linked to anthropogenic climate change in the semi-arid regions of the southwestern United States (US) is a serious concern¹. Multi-year droughts during the instrumental period² and decadal-length droughts of the past two millennia^{1,3} were shorter and climatically different from the future permanent, ‘dust-bowl-like’ megadrought conditions, lasting decades to a century, that are predicted as a consequence of warming⁴. So far, it has been unclear whether or not such megadroughts occurred in the southwestern US, and, if so, with what regularity and intensity. Here we show that periods of aridity lasting centuries to millennia occurred in the southwestern US during mid-Pleistocene interglacials. Using molecular palaeotemperature proxies⁵ to reconstruct the mean annual temperature (MAT) in mid-Pleistocene lacustrine sediment from the Valles Caldera, New Mexico, we found that the driest conditions occurred during the warmest phases of interglacials, when the MAT was comparable to or higher than the modern MAT. A collapse of drought-tolerant C₄ plant communities during these warm, dry intervals indicates a significant reduction in summer precipitation, possibly in response to a poleward migration of the subtropical dry zone. Three MAT cycles ~2 °C in amplitude occurred within Marine Isotope Stage (MIS) 11 and seem to correspond to the

mutated precessional cycles within this interglacial. In comparison with MIS 11, MIS 13 experienced higher precessional-cycle amplitudes, larger variations in MAT (4–6 °C) and a longer period of extended warmth, suggesting that local insolation variations were important to interglacial climatic variability in the southwestern US. Comparison of the early MIS 11 climate record with the Holocene record shows many similarities and implies that, in the absence of anthropogenic forcing, the region should be entering a cooler and wetter phase.

The hydroclimatology of the southwestern US shows significant natural variability including major historical droughts¹. Models of climate response to anthropogenic warming predict future dust-bowl-like conditions that will last much longer than historical droughts and have a different underlying cause, a poleward expansion of the subtropical dry zones⁴. At present, no palaeoclimatic analogues are available to assess the potential duration of aridity under a warmer climate or to evaluate its effect on the seasonality of precipitation.

Here we present a high-resolution climate record from an 82-m lacustrine sediment core (VC-3) from the Valles Caldera (Fig. 1) that spans two mid-Pleistocene glacial cycles from MIS 14 to MIS 10 (552 kyr ago to ~368 kyr ago; see Supplementary Information). MISs 11 and 13 are long interglacials that may have been as warm as

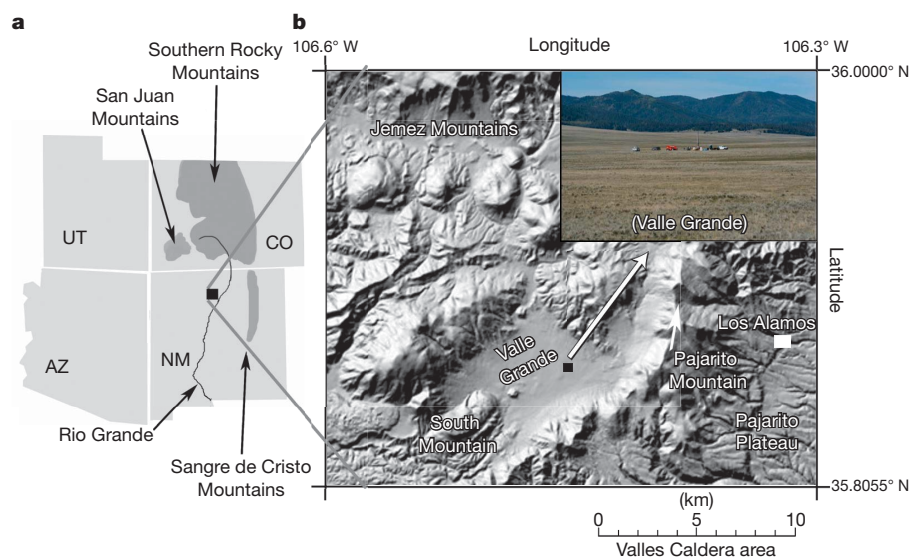


Figure 1 | Location map of the Valles Caldera. **a**, Location in northern New Mexico. **b**, Digital elevation model of the Valles Caldera showing the location of South Mountain rhyolite, Valle Grande, the drilling location of core VC-3 (black square) and a photograph of the drilling site.

¹Department of Earth & Planetary Sciences, University of New Mexico, Albuquerque, New Mexico 87131, USA. ²Large Lakes Observatory and Department of Chemistry and Biochemistry, University of Minnesota Duluth, Duluth, Minnesota 55812, USA. ³Large Lakes Observatory and Department of Geological Sciences, University of Minnesota Duluth, Duluth, Minnesota 55812, USA. ⁴Centre for Water Research, University of Western Australia, Crawley, Western Australia 6009, Australia. ⁵WA-Organic and Isotope Geochemistry Centre, Curtin University of Technology, Bentley, Western Australia 6845, Australia. ⁶School of Earth Sciences and Environmental Sustainability, Northern Arizona University, Flagstaff, Arizona 86011, USA. ⁷Laboratory of Paleocology, Bilby Research Center, Northern Arizona University, Flagstaff, Arizona 86011, USA. ⁸Earth and Environmental Sciences Division, EES-14, Los Alamos National Laboratory, Los Alamos, New Mexico 87545, USA. ⁹NIOZ Royal Netherlands Institute for Sea Research, Department of Marine Organic Biogeochemistry, PO Box 59, 1790 AB Den Burg, Netherlands. ¹⁰Department of Geological Sciences, Brown University, Providence, Rhode Island 02912, USA. ¹¹USGS Fort Collins Science Center, Jemez Mountains Field Station, Los Alamos, New Mexico 87544, USA.

the Holocene epoch, and MIS 11 is a good analogue for future natural climate variability with similar, low-amplitude precessional cycles^{6,7}. We used novel organic geochemical proxies (the cyclization ratio of branched tetraethers (CBT, related to pH) and the methylation index of branched tetraethers (MBT, related to temperature and pH^{5,8})) to reconstruct the annual MAT of the Valles Caldera watershed, and compared these with proxies of hydrologic balance to evaluate the relationship between warmth and aridity.

Interglacial MATs in the VC-3 record range from ~ 0 to 7°C , with the highest temperatures occurring in MIS 13 and early in MIS 11 (Fig. 2). The highest temperatures (5 – 7°C) are similar to modern MATs, of $\sim 5^\circ\text{C}$. The glacial stages have multiple millennial-scale temperature oscillations with amplitudes as large as 7°C ; approximately seven oscillations are preserved in MIS 12 (B1–B7), three in late MIS 14 (C1–C3) and one in early MIS 10 (A1). The frequency of these oscillations (2 – 10 kyr) is similar to those recorded in contemporaneous Atlantic Ocean sediment records⁹. All VC-3 stadials correlate with high percentages of *Picea* + *Abies* pollen, whereas interstadials have lower *Picea* + *Abies* pollen percentages and many correlate with local maxima in *Juniperus* and *Quercus* (Fig. 2). Increased percentages of Cyperaceae (sedge) pollen during several interstadials suggest a shallower lake rimmed by a broad marshy zone, which would have been minimized during stadials, when the lake was deeper. Interstadial shallowing probably resulted from increased evaporation and/or a reduction in the winter precipitation that dominates regional glacial-stage precipitation¹⁰.

Glacial terminations VI and V in the VC-3 record show temperature increases of ~ 7 and $\sim 8^\circ\text{C}$, respectively. The $\delta^{13}\text{C}$ record of TOC (Fig. 2) shows negative isotopic shifts of 2.5 – 3.5% at the terminations that we interpret as biotic responses to global increases in atmospheric CO_2 , similar to the Termination I $\delta^{13}\text{C}$ response in Lake Baikal¹¹.

We subdivide MIS 11 into five distinct substages, three warm and two cool, on the basis of MAT estimates, warm (lower-elevation) versus boreal (higher-elevation) pollen taxa, and variation in aquatic productivity proxies (Fig. 2). The warm substages (MISs 11a, c and e) are separated by intervals in which the temperature is $\sim 2^\circ\text{C}$ lower (MISs 11b and d). Although these small temperature variations are within the error limits of the MBT/CBT calibration, their timing is supported by decreases in warm pollen taxa and increases in boreal pollen taxa (with the exception of MIS 11a). The warmest substage, MIS 11e, occurs early in the interglacial, and has peak MATs of 6 – 7°C and the highest percentages of *Juniperus* pollen. After MIS 11e, the warm substages become progressively cooler.

The preservation of five MIS 11 substages in VC-3 is unusual. Most published records recognize only three substages, although a weak MIS 11e was noted in the Lake Baikal biogenic silica record¹² and there are three distinct (warm) peaks in MIS 11 pollen influx from Greenland preserved in ODP Site 646 sediments¹³. The VC-3 MIS 11a substage is cooler than the extended warm phases of MIS 11, similar to other mid-Pleistocene climate records¹², and is defined mainly by elevated lacustrine productivity (Si/Ti and TOC), more-positive $\delta^{13}\text{C}$ values, slightly higher temperature estimates and a combination of *Quercus*, *Picea* and *Abies* pollen that may not have a good modern climatic analogue. Within the limits of the VC-3 age model and the calibration uncertainty in the MBT/CBT proxies, the warm substages seem to correspond to the three precessional peaks of MIS 11, suggesting that the temperature response of this region to low-amplitude precessional cycles is $\sim 2^\circ\text{C}$. On the basis of the MIS 11 orbital forcing similarity with the Holocene, we suggest that in the absence of anthropogenic forcing future southwestern US climate should see a cooling of $\sim 2^\circ\text{C}$ relative to the early Holocene.

Large parts of MIS 13 seem to have been warmer than most of MIS 11, as shown by MATs of up to 7°C , higher *Juniperus* pollen percentages and the absence of *Picea* + *Abies* pollen (Fig. 2). Only MIS 11e had temperatures approaching the peak warmth of MIS 13. Other Northern Hemisphere records suggest that MIS 13 was warmer than

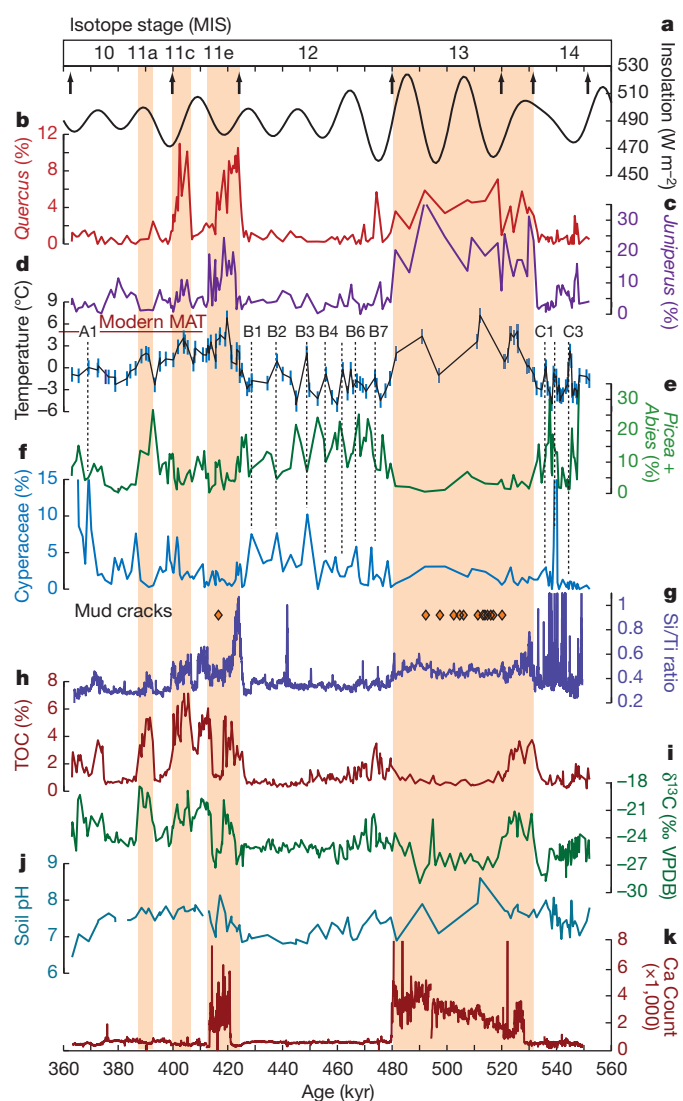


Figure 2 | Multi-proxy profiles of VC-3 plotted versus calendar age. Age model age–depth tie points are shown as arrows at the top and possible sedimentary hiatuses are indicated by positions of mud cracks (below). Shading indicates interglacial periods including odd-numbered MISs 11 and 13 and substages within MIS 11 (a, c and e). **a**, June insolation at latitude 30°N (ref. 6). **b**, *Quercus* (warm) pollen percentages. **c**, *Juniperus* (warm) pollen percentages. **d**, MAT estimates from MBT/CBT, with data size marker equivalent to 2°C (blue). Red line shows the modern MAT, of 4.8°C , in the Valle Grande. MBT/CBT temperature estimates have an absolute uncertainty of 5°C based on uncertainties in the global calibration (see further discussion in Supplementary Information). Millennial-scale events within the three glacial periods, defined by local maxima in MAT and Cyperaceae and local minima in *Picea* and *Abies*, are indicated (A for MIS 10, B for MIS 12 and C for MIS 14). **e**, *Picea* + *Abies* (boreal) pollen percentages. **f**, Cyperaceae pollen percentages; mud cracks indicated with orange diamonds. **g**, Si/Ti ratios from core scanning X-ray fluorescence (XRF). Large peaks in MIS 14 correspond to pumiceous gravels. **h**, Total organic carbon (TOC). **i**, $\delta^{13}\text{C}_{\text{TOC}} = ((^{13}\text{C}/^{12}\text{C})_{\text{sample}} / (^{13}\text{C}/^{12}\text{C})_{\text{standard}} - 1) \times 1,000\%$, relative to the Vienna PeeDee Belemnite (VPDB) standard. **j**, Watershed soil pH estimate from CBT. **k**, Calcium concentration in sediments from core scanning XRF.

MIS 11^{14,15}, and a smaller Greenland ice sheet¹³ and a lack of ice rafting in the North Atlantic⁹ also indicate Northern Hemisphere warmth during MIS 13, although not necessarily more than during MIS 11. In contrast, Southern Hemisphere records uniformly show a cooler MIS 13^{14,16}.

The higher MIS 13 temperatures in the southwestern US occur despite lower interglacial values of atmospheric CO_2 and CH_4 (ref. 17). However, the amplitude of precessional cycles and, hence, extremes in

Northern Hemisphere insolation were larger in MIS 13 than MIS 11⁶ and may have led to higher continental temperatures during parts of MIS 13. Temperature variability during MIS 13 was as much as 6 °C, which is significantly larger than that during MIS 11 (Fig. 2). In combination with the apparent precessional timing of MIS 11 warm sub-stages, this suggests that the southwestern US responded more strongly to insolation variations than to interglacial trends in greenhouse gases or global ice volume.

Mud cracks present in the warmest phases, MIS 11e and MIS 13, are unambiguous indicators of drier conditions. One 70-cm mud crack occurs within MIS 11e, and ~3 m of section within the upper portion of MIS 13 sediments contains multiple, centimetre-scale mud cracks, making this portion of the VC-3 age model less certain (Fig. 2). Also, the presence or absence of calcite in VC-3 sediments provides a continuous indicator of closed-basin or, respectively, open-basin conditions in the lake. No calcite precipitated during freshwater open-basin conditions, whereas during drier (closed-basin) conditions, evaporative concentration led to calcite precipitation and preservation. XRF core scanning results show two intervals with high calcium concentrations during MISs 11e and MIS 13 (Fig. 2) that correlate with elevated (1–2%) total inorganic carbon (not shown), whereas core sections with low calcium concentrations have essentially no total inorganic carbon. Significant increases in calcium mark the onsets of closed-basin conditions coincident with rapid temperature increases a few thousand years after Terminations V and VI (Fig. 2). Mud cracks develop later within these closed-basin periods.

Long-term changes in watershed hydrology are also reflected in the CBT-derived soil pH record. Changes in soil pH are assumed to reflect changes in total precipitation¹⁸; greater soil leaching and acidification occurs with more precipitation, whereas drier conditions result in weaker soil acidification. The most alkaline soils occur within the interglacial mud-cracked facies (Fig. 2) and are more basic for longer periods in MIS 13. In contrast, soil pH shows a progressive acidification through MIS 12, consistent with progressively wetter conditions through that glacial stage, and possibly also caused by increases in boreal tree vegetation.

During MIS 11e, Si/Ti (a proxy for diatom productivity) is initially very high and then declines to average interglacial values, whereas TOC increases to ~5% in MIS 11e and is also high during early MIS 11d and MISs 11c and 11a. After the glacial termination, $\delta^{13}\text{C}_{\text{TOC}}$ rapidly increases to ~–20‰, indicating an expansion of *C*₄ plants in the watershed and higher lacustrine productivity levels¹⁹. Increases $\delta^{13}\text{C}_{\text{TOC}}$ also occurs in MISs 11c and 11a, and early in MIS 11d. Continued high Si/Ti, TOC and more-positive $\delta^{13}\text{C}_{\text{TOC}}$ values during early stages of closed-basin conditions in MIS 11e and MIS 13 indicate periods of robust summer precipitation and productivity related to insolation forcing of monsoon strength, even as reduced winter precipitation led to less precipitation overall and closed-basin conditions.

Mud-cracked facies in MIS 11e and MIS 13 are characterized by negative shifts in $\delta^{13}\text{C}_{\text{TOC}}$ of 6–7‰ and dramatic decreases in percentage TOC (Fig. 2). Si/Ti ratios, however, remain elevated relative to glacial values, suggesting that low percentage TOC values are due to organic degradation in shallow, oxidized sediments rather than lower aquatic productivity. The large negative shifts in $\delta^{13}\text{C}_{\text{TOC}}$ are best explained by a collapse of the interglacial *C*₄ plant community. Variations in *C*₃ and *C*₄ plant communities are a complex function of temperature, atmospheric CO₂, and growing-season precipitation^{20,21}. These dry intervals include some of the highest MATs in the VC-3 record that should favour *C*₄ plants, and the relatively high interglacial levels of atmospheric CO₂ during MISs 11 and 13 vary by less than 20–30 p.p.m.v. Thus, the best explanation for the decline of *C*₄ plants in the watershed is a significant decrease in summer precipitation. In contrast to the early interglacial closed-basin phases where significant *C*₄ plant growth provided evidence for robust summer precipitation, we interpret the extended arid periods later in MIS 11e and MIS 13 to be the result of greatly reduced summer precipitation.

Following the aridity of MIS 11e, the lake expanded during MIS 11d as shown by well-laminated sediments and open-basin conditions (low calcium values). Despite this interval being ~2 °C cooler, sufficient summer rainfall early in MIS 11d allowed renewed *C*₄ plant growth.

Northern New Mexico at present receives ~40–50% of its annual precipitation total during the summer monsoon²². During the warmest phases of the interglacials, we would expect greater summer precipitation, as the monsoon is primarily driven by land surface heating²². Indeed, linkages among interglacial warmth, robust summer precipitation and precessional variations are indicated by the presence of *C*₄ plants in early MIS 13, early MIS 11e and MISs 11c and 11a, when MATs were similar to or slightly less than modern values, but the warmest intervals did not have robust summer precipitation. As possible analogues for interglacial aridity, both historical droughts and pre-historical megadroughts were characterized by reductions in winter precipitation as a consequence of more-frequent La Niña events^{2,3,23}, with summer precipitation reduced also.

In contrast, the extended arid episodes (centuries to millennia) of MIS 11e and MIS 13 lasted much longer than pre-historical megadroughts. An analogous relationship between peak interglacial warmth and extended aridity was also noted in a mid-Holocene bog record from the margin of the Valles Caldera²⁴. Here, ~2 kyr of desiccation occurred contemporaneously with the highest temperatures of the Holocene in the southwestern US²⁵ and with the northernmost extent of the inter-tropical convergence zone in the Gulf of Mexico²⁶. The timing of this dry episode in the Holocene interglacial following the deglaciation is very similar to that of the arid episode in MIS 11e; subsequent late-Holocene conditions became wetter in the southwestern US, with increased winter precipitation²⁷ similar in timing to wetter conditions during MIS 11d in the VC-3 record.

The strong correspondence between the warmest temperatures and extended aridity during at least three interglacials (MIS 13, MIS 11e and the early Holocene) in the southwestern US suggests a stable climate state fundamentally different from conventional drought conditions. These periods of aridity are related to lower winter precipitation (as mid-latitude westerlies shifted polewards during warmer periods), but reductions in summer precipitation seem to be critical to their development. Unlike the temporary summer blocking high over the southwestern US thought to partly explain the 1950s drought²⁸, these longer periods of aridity indicate a more permanent change in atmospheric circulation. Climate model analysis shows that the dust-bowl-like conditions predicted for the southwestern US over the next century in response to anthropogenic warming arise from a poleward shift of the mid-latitude westerlies and the poleward branch of the Hadley cell⁴. This response to warming is not transient and would result in a more arid southwestern US as long as the underlying conditions (warming) remained in place. Our palaeoclimate record shows that extended interglacial aridity is strongly linked to higher-than-modern temperatures and reduced summer rainfall, and we suggest that a similar expansion of the subtropical dry zone has occurred several times in the past in response to natural warming, even though MIS 11 and MIS 13 had different orbital and atmospheric CO₂ forcings. Our results strongly indicate that interglacial climates in the southwestern US can experience prolonged periods of aridity, lasting centuries to millennia, with profound effects on water availability and ecosystem composition. The risk of prolonged aridity is likely to be heightened by anthropogenic forcing^{1,4}.

METHODS SUMMARY

Measurement of fossil branched glycerol dialkyl glycerol tetraether (GDGT) membrane lipids from soil bacteria were conducted at the Royal Netherlands Institute for Sea Research (NIOZ) and Brown University following procedures outlined in Supplementary Information. At NIOZ we analysed GDGTs on an Agilent 1100 series LC-MSD SL, and at Brown University we analysed GDGTs on an HP 1200 series LC-MS. Both labs used an Alltech Prevail Cyano column (2.1 × 150 mm, 3 μm) with the same solvent elution scheme and instrument operating conditions. GDGTs were detected using atmospheric-pressure chemical ionization mass spectrometry. All

liquid chromatography/mass spectrometry runs were integrated at NIOZ by the same technician to ensure consistency. To evaluate the compatibility between the Brown and NIOZ measurements, representative samples were analysed on both machines and the resulting MBT/CBT indices were found to be identical within analytical uncertainty.

Processing for pollen included suspension in KOH, dilute HCL, hydrofluoric acid and acetolysis solution. The pollen sum included all terrestrial pollen types; Cyperaceae percentages were calculated outside the sum. We identified pollen grains to the lowest taxonomic level using the modern pollen reference collection at Northern Arizona University. Analysis for organic carbon elemental concentrations and $\delta^{13}\text{C}_{\text{TOC}}$ included samples being dried, ground and pretreated twice with 6 N HCL at 60 °C to remove the carbonate fraction. TOC and $\delta^{13}\text{C}_{\text{TOC}}$ were analysed using a Costech Elemental Analyser coupled to a Thermo-Finnigan Delta Plus isotope ratio mass spectrometer. The bulk elemental composition of core VC-3 sediments was determined using an ITRAX X-ray Fluorescence Scanner (Cox Analytical Instruments). XRF scanning was conducted at 1-cm resolution with 60-s scans using a molybdenum X-ray source set to 30 kV and 15 mA.

Received 11 June 2010; accepted 12 January 2011.

- Woodhouse, C. A. *et al.* A 1,200-year perspective of 21st century drought in southwestern North America. *Proc. Natl Acad. Sci. USA* **107**, 21283–21288 (2010).
- McCabe, G. J., Palecki, M. A. & Betancourt, J. L. Pacific and Atlantic Ocean influences on multidecadal drought frequency in the United States. *Proc. Natl Acad. Sci. USA* **101**, 4136–4141 (2004).
- Cook, E. R., Seager, R., Cane, M. A. & Stahle, D. W. North American drought: reconstructions, causes and consequences. *Earth Sci. Rev.* **81**, 93–134 (2007).
- Seager, R. *et al.* Model projections of an imminent transition to a more arid climate in southwestern North America. *Science* **316**, 1181–1184 (2007).
- Weijers, J. W. H., Schouten, S., van den Donker, J. C., Hopmans, E. C. & Sinninghe Damsté, J. S. Environmental controls on bacterial tetraether membrane lipid distribution in soils. *Geochim. Cosmochim. Acta* **71**, 703–713 (2007).
- Berger, A. & Loutre, M. F. Insolation values for the climate of the last 10 million years. *Quat. Sci. Rev.* **10**, 297–317 (1991).
- Loutre, M. F. & Berger, A. Marine Isotope Stage 11 as an analog for the present interglacial. *Global Planet. Change* **36**, 209–217 (2003).
- Weijers, J. W. H., Schefuß, E., Schouten, S. & Sinninghe Damsté, J. S. Coupled thermal and hydrological evolution of tropical Africa over the last deglaciation. *Science* **315**, 1701–1704 (2007).
- McManus, J. F., Oppo, D. W. & Cullen, J. L. A 0.5-million-year record of millennial-scale climate variability in the North Atlantic. *Science* **283**, 971–975 (1999).
- Kutzbach, J. E. *et al.* Climate and biome simulation for the past 21000 years. *Quat. Sci. Rev.* **17**, 473–509 (2000).
- Prokopenko, A. A., Williams, D. F., Karabanov, E. B. & Khursevich, G. K. Response of Lake Baikal ecosystem to climate forcing and pCO₂ change over the Last Glacial/Interglacial transition. *Earth Planet. Sci. Lett.* **172**, 239–253 (1999).
- Prokopenko, A. A. *et al.* Muted climate variations in continental Siberia during the mid-Pleistocene epoch. *Nature* **418**, 65–68 (2002).
- de Vernal, A. & Hillaire-Marcel, C. Natural variability of Greenland climate, vegetation, and ice volume during the past million years. *Science* **320**, 1622–1625 (2008).
- Guo, Z. T., Berger, A., Yin, Q. Z. & Qin, L. Strong asymmetry of hemispheric climates during MIS-13 inferred from correlating China loess and Antarctic ice records. *Clim. Past* **5**, 21–31 (2009).
- Rosignol-Strick, M., Paterne, M., Bassinot, F. C., Emeis, K. C. & De Lange, G. J. An unusual mid-Pleistocene monsoon period over Africa and Asia. *Nature* **392**, 269–272 (1998).
- Jouzel, J. *et al.* Orbital and millennial Antarctic climate variability over the past 800,000 years. *Science* **317**, 793–796 (2007).
- Loulergue, L. *et al.* Orbital and millennial-scale features of atmospheric CH₄ over the past 800,000 years. *Nature* **453**, 383–386 (2008).
- Johnson, D. W., Hanson, P. J., Todd, D. E., Susfalk, R. B. & Trettin, C. F. Precipitation change and soil leaching: field results and simulations from Walker Branch Watershed, Tennessee. *Wat. Air Soil Pollut.* **105**, 251–262 (1998).
- Meyers, P. A. Applications of organic geochemistry to paleolimnological reconstructions: a summary of examples from the Laurentian Great Lakes. *Org. Geochem.* **34**, 261–289 (2003).
- Ehleringer, J. R., Cerling, T. E. & Helliker, B. R. C₄ photosynthesis, atmospheric CO₂ and climate. *Oecologia* **112**, 285–299 (1997).
- Huang, Y. *et al.* Climate change as the dominant control on glacial-interglacial variations in C₃ and C₄ plant abundance. *Science* **293**, 1647–1651 (2001).
- Douglas, M. W., Maddox, R. A., Howard, K. & Reyes, S. The Mexican monsoon. *J. Clim.* **6**, 1665–1677 (1993).
- Schubert, S. D., Suarez, M. J., Pegion, P. J., Koster, R. D. & Bacmeister, J. T. On the cause of the 1930s dust bowl. *Science* **303**, 1855–1859 (2004).
- Anderson, R. S. *et al.* Development of the mixed conifer forest in northern New Mexico and its relationship to Holocene environmental change. *Quat. Res.* **69**, 263–275 (2008).
- Jiménez-Moreno, G., Fawcett, P. J. & Anderson, R. S. Millennial- and centennial-scale vegetation and climate changes during the Late Pleistocene and Holocene from northern New Mexico (USA). *Quat. Sci. Rev.* **27**, 1448–1452 (2008).
- Poore, R. Z., Pavich, M. J. & Grissino-Mayer, H. D. Record of the North American southwest monsoon from Gulf of Mexico sediment cores. *Geology* **33**, 209–212 (2005).
- Enzel, Y., Cayan, D. R., Anderson, R. Y. & Wells, S. G. Atmospheric circulation during Holocene lake stands in the Mojave Desert: evidence of regional climate change. *Nature* **341**, 44–47 (1989).
- Namias, J. Some meteorological aspects of drought with special reference to the summers of 1952–54 over the United States. *Mon. Weath. Rev.* **83**, 199–205 (1955).

Supplementary Information is linked to the online version of the paper at www.nature.com/nature.

Acknowledgements We thank A. Mets for analytical support, W. McIntosh for the Ar–Ar age determination, T. Wawrzyniec and A. Ellwein for drilling help, and the Valles Caldera Trust for permission to drill in the Valle Grande. Core assistance was provided by LRC/LacCore. This work was supported by the NSF Paleoclimate and P2C2 programs, IGPP LANL and the USGS Western Mountain Initiative. Support from the Gledden Fellowship is acknowledged. This work forms contribution 2399-JW at the Centre for Water Research, The University of Western Australia and contribution 131 at the Laboratory of Paleocology, Northern Arizona University.

Author Contributions Writing and interpretation was done by P.J.F. with significant contributions from J.P.W., R.S.A., J.M.H. and E.T.B. MBT/CBT analyses were conducted by J.P.W., M.A.B., J.S.S.D., S.S., Y.H. and J.T. Organic carbon/nitrogen analyses were conducted by P.J.F., J.M.H., L.M.C.-D., J.F. and V.A. XRF core scanning analyses were conducted by E.T.B. Pollen analyses and palaeovegetation analyses were conducted by R.S.A., S.J.S. and C.D.A., and F.G., G.W. and P.J.F. conducted core sediment and stratigraphic analyses. L.D.-H. and J.W.G. investigated palaeomagnetic and rock magnetic core properties. All authors discussed the results and commented on the manuscript.

Author Information Reprints and permissions information is available at www.nature.com/reprints. The authors declare no competing financial interests. Readers are welcome to comment on the online version of this article at www.nature.com/nature. Correspondence and requests for materials should be addressed to P.J.F. (fawcett@unm.edu).